

Quantum Key Distribution Overcoming Extreme Noise: Simultaneous Subspace Coding Using High-Dimensional Entanglement

Mirdit Doda^{1,2}, Marcus Huber^{2,3,4}, Gláucia Murta⁵, Matej Pivoluska⁶, Martin Plesch^{1,6,*}, and Chryssoula Vlachou^{7,8}

¹*Institute of Physics, Slovak Academy of Sciences, Bratislava 845 11, Slovakia*

²*Institute for Quantum Optics and Quantum Information—IQOQI Vienna, Austrian Academy of Sciences, Boltzmannngasse 3, Vienna 1090, Austria*

³*Institute for Atomic and Subatomic Physics, Vienna University of Technology, Vienna, Austria*


⁴*Vienna Center for Quantum Science and Technology, Atominsitut, TU Wien, Vienna 1020, Austria*

⁵*Institut für Theoretische Physik III, Heinrich-Heine-Universität Düsseldorf, Universitätsstraße 1, Düsseldorf D-40225, Germany*

⁶*Institute of Computer Science, Masaryk University, Brno 602 00, Czech Republic*

⁷*Instituto de Telecomunicações, Av. Rovisco Pais 1, Lisboa 1049-001, Portugal*

⁸*Departamento de Matemática, Instituto Superior Técnico, Universidade de Lisboa, Av. Rovisco Pais 1, Lisboa 1049-001, Portugal*

 (Received 30 April 2020; revised 25 January 2021; accepted 27 January 2021; published 1 March 2021)

High-dimensional entanglement promises to increase the information capacity of photons and is now routinely generated, exploiting spatiotemporal degrees of freedom of single photons. A curious feature of these systems is the possibility of certifying entanglement despite strong noise in the data. We show that it is also possible to exploit this noisy high-dimensional entanglement for quantum key distribution by introducing a protocol that uses multiple subspaces of the high-dimensional system simultaneously. Our protocol can be used to establish a secret key even in extremely noisy experimental conditions, where qubit protocols fail. To show that, we analyze the performance of our protocol for noise models that apply to the two most commonly used sources of high-dimensional entanglement: time bins and spatial modes.

DOI: [10.1103/PhysRevApplied.15.034003](https://doi.org/10.1103/PhysRevApplied.15.034003)

I. INTRODUCTION

Quantum communication is one of the most mature areas of quantum technologies, with quantum key distribution (QKD) [1–5] as its most prominent example. QKD is a cryptographic primitive allowing two parties, Alice and Bob, to securely establish a shared secret key in the presence of an adversary, Eve.

One of the primary scientific challenges in the transition to commercial QKD applications is the relatively low key rate and the high susceptibility to noise. Contrary to classical communication with light, the information encoded in quantum states can neither be copied nor amplified, meaning that only a few photons survive long-distance transmission. Furthermore, single photons are challenging to detect and hard to isolate, leading to a lot of noise in the data.

The problem of successfully performing a QKD protocol over noisy channels is also connected with the basic

task of distributing entanglement. Essentially, if the channel is too noisy to distribute entanglement, it is also too noisy for QKD [3,5]. This correspondence points to a possible solution to the above challenges—the use of QKD protocols that utilize high-dimensional (HD) entanglement. HD entanglement is known to feature high resistance to noise according to theoretical noise models (e.g., white noise). At the same time, HD states can encode more bits per photon. Another reason for considering entanglement-based QKD protocols is that they are less prone to practical attacks [6] compared to their prepare-and-measure counterparts, thus also providing higher practical security. Indeed, using entanglement based systems, one can relinquish trust in the source and place it in the hands of an untrusted node. Furthermore, entanglement distribution is a necessary step toward (partially) device-independent implementations. Currently, HD QKD protocols are becoming practical, because HD quantum states of entangled photons can be routinely produced in the laboratory using temporal [7–22], frequency encoding [23,24], or multiple ones simultaneously in a so-called hyperentangled state [25–29].

*plesch@savba.sk

Unfortunately, putting this idea into practice is not straightforward, as the physical nature of the carriers and the actual noise become very important. HD quantum systems are not as easily controlled and measured as polarization qubits and all implementations come with their own limitations and additional sources of noise. While used for proof-of-principle experiments in QKD before [30–53], they have never been competitors to regular qubit encoding and the majority of practical QKD implementations still use binary encoding of quantum states in photons, such as polarization [54] or time-bin qubits [55]. In fact, perhaps surprisingly, even the theoretically predicted higher noise resistance of HD entanglement has only recently been demonstrated in *realistic scenarios* [56]. There, the data obtained from measuring HD states distributed over realistic very noisy channels can be used to certify the presence of entanglement. However, such noisy data are not necessarily useful for QKD. This is because correction of the errors on the outcomes obtained using multiple-outcome measurements is more demanding than the correction of binary outcomes and it conventionally comes at a cost that can obliterate the advantage of using HD entanglement. Hence, the question of whether such noisy HD entanglement can actually be useful remains open. In other words, ‘*can we still harness the HD nature of entanglement in situations where noise dominates the signal and qubit-based QKD would be impossible?*’ In this work, we answer that question in the affirmative and provide an entanglement-based HD QKD protocol with *simultaneous subspace coding*. We provide detailed noise models for two paradigmatic implementations of HD entanglement to showcase the suitability of our protocol for practical advantages in QKD.

II. THE PROTOCOL

The general idea is to use a $(d \times d)$ -dimensional entangled quantum system to perform multiple instances of a QKD protocol simultaneously in nonoverlapping subspaces. The choice of subspaces is arbitrary but to simplify the notation we formulate the protocol using subspaces of equal size k . The protocol requires two measurement settings—the computational-basis measurement and a measurement in a basis mutually unbiased with respect to the computational in each subspace of size k . Therefore, let $\{A_1^x\}_{x=0}^{d-1}$ and $\{B_1^y\}_{y=0}^{d-1}$ denote the projectors on the computational basis of \mathcal{H}_A and \mathcal{H}_B , respectively, and let $\{A_2^x\}_{x=0}^{d-1}, \{B_2^y\}_{y=0}^{d-1}$ be a tensor product of projectors on the mutually unbiased basis vectors in subspaces of size k (see Appendix A for details). Alice’s measurement outcome $x = mk + i$ is interpreted as outcome i in the m th subspace. Bob’s measurement outcome y is interpreted analogously.

The protocol consists of the following steps:

Protocol 1 Subspace QKD

- 1: **Distribution.** A source distributes a state ρ_{AB} to Alice and Bob.
 - 2: **Measurement.** Upon receiving the state, Alice and Bob choose independently at random bits w_A and w_B , respectively, such that $p(w_A = 1) = p(w_B = 1) = \varepsilon \ll 1$. If $w_A = 0$, Alice performs a measurement in the $\{A_1^x\}_{x=0}^{d-1}$ basis, otherwise she measures in $\{A_2^x\}_{x=0}^{d-1}$. Similarly, Bob measures his part of the state in $\{B_1^y\}_{y=0}^{d-1}$ or $\{B_2^y\}_{y=0}^{d-1}$, accordingly. They record the outcomes x and y in the register X and Y , respectively. Steps 1 and 2 are repeated N times.
 - 3: **Sifting and subspace selection.** Through a classical public authenticated channel, Alice and Bob reveal for each iteration their basis choice and the values m_A and m_B of the subspaces that their outcomes belong to.
 - (a) If $m_A = m_B = m$ and $w_A = w_B$, Alice and Bob set $M = m$, $x' = x - mk$ and $y' = y - mk$.
 - (b) If $m_A \neq m_B$ or $w_A \neq w_B$, they set $M = \perp$, $x' = y' = \perp$, and discard the round.
 - 4: **Parameter estimation.** Alice and Bob use the second measurement-basis outcomes (*test rounds*) and some of the key first measurement-basis outcomes (*generation rounds*) to estimate correlations for each block $M = m$. The remaining measurement results form the raw key.
 - 5: **Information reconciliation and privacy amplification.** Alice and Bob proceed with information reconciliation and privacy amplification in each subspace and extract the final key.
-

To assess the efficiency of the protocol, we calculate the achievable key rate K in the asymptotic limit. Initially, we assume that Eve is restricted to *collective attacks*, i.e., at each iteration she attacks identically and independently of the previous, and she can perform a measurement on her ancillary system at any future time. This assumption can be dropped later with a de Finetti–type argument [57,58] and thus security against any *general coherent attack* can be obtained. Note that since we derive our results in the asymptotic setting, we can safely use the de Finetti theorem without degrading the key-rate expression. Furthermore, we assume that Eve prepares the entangled states that Alice and Bob share. Proving security under this assumption implies security for any implementation of the protocol. Besides these security assumptions, we also assume a detector model with fair sampling and access of the legitimate parties to randomness and to a classical public authenticated channel, as is usual in QKD protocols. Under these assumptions, the asymptotic key rate is given by [59,60] $K \geq H(X|E_T) - H(X|Y)$, where $H(X|E_T)$ is the von Neumann entropy of Alice’s key round outcome X , conditioned on the total information available to the

eavesdropper Eve at the end of Step 4, given that Eve holds a purification of the state ρ_{AB} , and $H(X|Y)$ is the conditional Shannon entropy between Alice's and Bob's key-round outcomes.

The asymptotic key rate of Protocol 1 is given by

$$K_{\text{tot}} \geq \sum_{m=0}^{\ell-1} P(M=m)K_m, \quad (1)$$

where $P(M=m)$ is the probability that both Alice and Bob obtain an outcome in subspace m and K_m is the corresponding rate, given by $K_m = H(X'|E_T)_{\tilde{\rho}^m} - H(X'|Y')_{\tilde{\rho}^m}$, where $\tilde{\rho}^m$ is the state effectively shared by the parties in the subspace m . The proof of Eq. (1) is based on techniques similar to those used in protocols with advantage distillation [61–64]. For the definition of the state $\tilde{\rho}^m$ and the detailed proof of this result, see Appendix A.

To compute K_m for the subspace m , we lower bound the conditional entropy $H(X'|E_T)_{\tilde{\rho}^m}$ by the conditional minimum entropy: $H(X'|E_T)_{\tilde{\rho}^m} \geq H_{\min}(X'|E_T)_{\tilde{\rho}^m}$, where $H_{\min}(X'|E_T)_{\tilde{\rho}^m} = -\log P_g^m$ and P_g^m is the average probability that Eve can guess Alice's outcome computed using the effective state $\tilde{\rho}^m$. To determine P_g^m , for a subspace m from measurement results, we use the correlations of Alice's and Bob's outcomes in the second basis, expressed as

$$W_k^m = \sum_{i=0}^{k-1} P(ii|22, m), \quad (2)$$

where $P(ii|22, m) = [P(x = mk + i, y = mk + i|22)/P(M = m)]$ is the probability that Alice and Bob obtain equal outcomes when they measure in $\{A_2^x\}_{x=0}^{d-1}$ and $\{B_2^y\}_{y=0}^{d-1}$ and obtain outcomes in the subspace m . In Appendix B, we present and solve the optimization problem that enables us to show that Eve's guessing probability for the subspace m can be expressed as a function of the subspace dimension k and the correlation W_k^m , as

$$H_{\min}(X'|E_T)_{\tilde{\rho}^m} = -\log_2 \left(\frac{(\sqrt{W_k^m} + \sqrt{(k-1)(1-W_k^m)})^2}{k} \right). \quad (3)$$

The conditional entropy $H(X'|Y')_{\tilde{\rho}^m}$ for subspace m can be estimated directly from the measurement outcomes in the basis $\{A_1^x\}_{x=0}^{d-1}$ and $\{B_1^y\}_{y=0}^{d-1}$.

Note that a similar technique of subspace encoding has been used previously to encode qubits using HD systems [43,44]. However, our protocol is intrinsically different. Our construction allows us to explore subspaces of arbitrary sizes and the encoding is simultaneous in all the subspaces. Moreover, our protocol, as well as the noise analyses presented in the following sections, are designed for an entanglement-based implementation, which offers a

higher level of practical security compared to prepare-and-measure protocols, the noise robustness and feasibility of which have been considered in Ref. [45].

A. Isotropic state example

First we investigate a paradigmatic noise model, i.e., a maximally entangled state mixed with white noise, $\rho_d(v) = v|\psi_d^+\rangle\langle\psi_d^+| + [(1-v)/d^2]\mathbb{1}_d \otimes \mathbb{1}_d$ with visibility v . We calculate the asymptotic key rate for $k = d$, i.e., Alice and Bob use standard QKD and derive the key from the full Hilbert space. Measuring $\rho_d(v)$ in the second basis for both Alice and Bob leads to $W_d = v + (1-v/d)$ and thus via Eq. (3) $H(X|E_T) \geq -\log_2 \left(\frac{(\sqrt{vd+1-v} + (d-1)\sqrt{1-v})^2}{d^2} \right)$. To determine $H(X|Y)$, we observe that, given $\rho_d(v)$, the probability distribution for Alice obtaining result x and Bob obtaining result y in the key rounds is given by $P_{\text{key}}(xy) = v(\delta_{xy}/d) + (1-v/d^2)$ and the respective conditional probability distribution is $P_{\text{key}}(x|y) = v\delta_{xy} + (1-v/d)$.

Similar calculations can be done in the case in which Alice and Bob perform Protocol 1 with subspaces $\mathcal{H}_{A_m} \otimes \mathcal{H}_{B_m}$ of size $k \times k$. In such a case, they effectively measure the state $\rho_k^m(\tilde{v})$ in each subspace m , which can be obtained by projecting $\rho_d(v)$ onto this subspace. Because of the symmetry of $\rho_d(v)$, the state $\rho_k^m(\tilde{v})$ is independent of m and its density matrix is equivalent to $\rho_k(\tilde{v}) = \tilde{v}|\psi_k^+\rangle\langle\psi_k^+| + [(1-\tilde{v})/k^2]\mathbb{1}_k \otimes \mathbb{1}_k$, where $|\psi_k^+\rangle = (1/\sqrt{k}) \sum_{i=0}^{k-1} |ii\rangle$ and $\tilde{v} = \tilde{v}(d, v, k) := vd/(vd+k-vk)$.

For each subspace $H(X'|E_T)_{\tilde{\rho}^m}$ and $H(X'|Y')_{\tilde{\rho}^m}$, we can now set $\tilde{\rho}^m = \rho_k(\tilde{v})$. Measurements of this state in the second basis lead to $W_k^m = (vd+1-v/vd+k-vk)$, which [using Eq. (3)] results in

$$H(X'|E_T)_{\tilde{\rho}^m} \geq -\log_2 \left(\frac{(\sqrt{vd+1-v+(k-1)\sqrt{1-v}})^2}{k(vd+k-vk)} \right). \quad (4)$$

Evaluating $H(X'|Y')_{\rho_k(\tilde{v})}$ and summing over all subspaces leads to

$$\begin{aligned} K_{\text{tot}}^{\text{iso}}(d, v, k) &\geq \left(\frac{vd+k-vk}{d} \right) \log_2 \left(\frac{k}{(\sqrt{vd+1-v+(k-1)\sqrt{1-v}})^2} \right) \\ &\quad + \left(\frac{vd+1-v}{d} \right) \log_2(vd+1-v) \\ &\quad + \left(\frac{(k-1)(1-v)}{d} \right) \log_2(1-v). \end{aligned} \quad (5)$$

For each d and v , which are known experimental parameters, one can optimize $K_{\text{tot}}^{\text{iso}}(d, v, k)$ over the subspace size k to determine the protocol implementation with the optimal key rate. Another interesting quantity is the critical visibility, i.e., the visibility beyond which one can no longer obtain a positive key rate. This is generally a complicated function of k and d . However, considering even d and $k = 2$, it can be shown that the key rate

is positive for $v > (1/1 + 0.0893d)$. For constant v , one can always obtain a positive key rate by increasing the global dimension d . This is in accordance with the previously observed fact—the robustness of entanglement in the isotropic state increases with the dimension. In practice, however, the v is not a constant but, rather, a function of d and strongly depends on the particular implementation. To infer whether our protocol actually holds the potential to outperform qubit-based protocols, it is thus essential to take the experimental specifications into account. In what follows, we study two different state-of-the-art implementations of our protocol with dimension-dependent noise models. The first employs temporal and the second spatial degrees of freedom of photons for the generation of HD entanglement. The motivation for using these particular setups is that they have recently been shown to provide an advantage for entanglement certification [56].

III. REALISTIC NOISE MODELS

A. Implementation using temporal degrees of freedom

To start with the temporal implementation, we consider a hyperentangled state of the form $|\Psi\rangle = |\phi^-\rangle_{AB} \otimes \int dt f(t) |t\rangle_A \otimes |t\rangle_B$. The part of the state entangled in energy-time space is produced by a laser source via spontaneous parametric down-conversion and the interference of photons in the temporal domain is subsequently enabled by introducing entanglement in polarization by means of $|\phi^-\rangle_{AB}$. Alice and Bob measure the time of arrival, t , of the photons, i.e., the time when the detectors click. The maximum resolution with which they can detect photons arriving at the same time is given by the duration of a time bin, t_b , and with respect to it, they determine a time frame, F , outside of which any photon that arrives is considered “lost.” They choose $F = dt_b$ for $d \in \mathbb{N}$, effectively discretizing the energy-time space to obtain a space of dimension d ; the encoding space. The frames in which they both have one click are postselected and used for the key rate. In Appendix C, we present in detail a noise model for this setup, in which we take into account noise effects due to the interaction of the photons with the environment and due to the imperfect detectors. In particular, photons might be lost before arriving in the laboratory and other photons coming from the environment might enter and make the detectors click. The environmental photons are the main source of noise for this implementation. Moreover, we consider dark counts, i.e., detector clicks in the absence of a photon and, finally, that the detectors might not click in the presence of a photon. We can, then, express the key rate as a function of the dimension d and the visibility v , which is the probability that, given that both Alice and Bob have one click, this click is due to a photon coming from the laser source and not due to an environmental photon or a

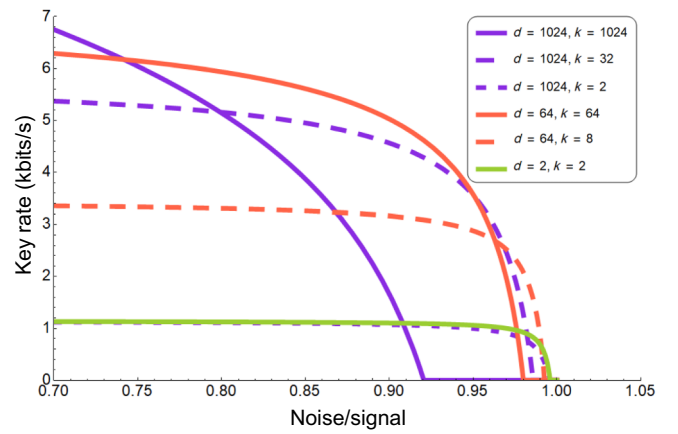


FIG. 1. The achievable key rate versus the signal-to-noise ratio for the temporal domain. The signal-to-noise ratio is the average number of nonentangled photons that arrive in the laboratory (including singles and taking into account detector inefficiencies) divided by the overall average number of clicks per second, assuming that these quantities are the same for both parties. For this implementation, this quantity is dimension independent. Since we vary the frame sizes but not the bin sizes, the end points are independent of the total dimension and the optimal noise resistance is always achieved in two-dimensional subspaces, which includes the traditional qubit encoding ($d = 2, k = 2$). The plot illustrates the fact that choosing $k > 2$, however, can significantly increase the total key rate at lower noise levels. Another fact one can directly observe is that the best key rate for a given noise level can be obtained by fine tuning values of d and k .

dark count. For this model, the visibility is given as

$$v(d) = 1/(1 + dt_b T_A T_B \gamma^{-1}) \quad (6)$$

and the production rate of postselected frames/s is

$$R(d, v) = e^{-d t_b (T_A + T_B + \gamma)} (d t_b T_A T_B + \gamma), \quad (7)$$

where $T_{A/B}$ and γ are experimental parameters incorporating all quantities that are independent of d . $T_{A/B}$ is the average number of uncorrelated clicks per second, coming from dark counts, environmental photons or laser photons when one of the parties is affected by losses or detector inefficiencies; γ is the average number of detected entangled photons per second, i.e., the photons coming from the laser source that are not lost and produce a click. The achievable key rate expressed in bits/s is $K(d) = R(d, v) K_{\text{tot}}^{\text{iso}}(d, v, k)$. In practical implementations, this number is further multiplied by $(1 - \varepsilon)^2$, i.e., the probability that both Alice and Bob use the first measurement. Since here we are dealing with the asymptotic key rate, we can choose ε arbitrarily close to 0, hence we disregard it. In Fig. 1, we plot $K(d)$ versus the signal-to-noise ratio for different subspace-dimension choices k in various total dimensions d .

B. Implementation using spatial degrees of freedom

We move to photons entangled in spatial degrees of freedom. Due to spatial symmetry, the state produced by the laser source is of the form $|\Psi\rangle = \sum_{l=-\infty}^{\infty} c_l |l\rangle_A |-l\rangle_B$, where l denotes momentum modes and c_l depends on the source specifications. This state is subsequently projected in a space spanned by a finite subset of modes, l , with cardinality d ; our encoding space hence arises from an effective discretization with respect to the finite resolution of the detectors. In our noise model, we consider noise effects originating from losses, environmental photons, detector inefficiencies, and dark counts. For the key rate, Alice and Bob postselect the rounds in which they both obtain one click and, just as in the previous implementation, the visibility v includes the rounds where the clicks come from a source photon pair. In this implementation, each party needs a detector *for each mode*, resulting in dark counts contributing the most to noise through more frequent accidental coincidences. We calculate the visibility to be

$$v(d) = \frac{e^{\frac{\gamma}{d}} - 1}{e^{\frac{\gamma}{d}} - 1 + d \left[1 - e^{-\left(\mu^A + \frac{\xi^A}{d}\right)} \right] \left[1 - e^{-\left(\mu^B + \frac{\xi^B}{d}\right)} \right]}, \quad (8)$$

and the rate of postselected rounds/s is given by

$$R(d, v) = C e^{-d(\mu^A + \mu^B)} e^{\frac{(\xi^A + \xi^B)}{d}} \times \left\{ d^2 \left[1 - e^{-\mu^A - \frac{\xi^A}{d}} \right] \left[1 - e^{-\mu^B - \frac{\xi^B}{d}} \right] + d \left(e^{\frac{\gamma}{d}} - 1 \right) \right\}, \quad (9)$$

where $\mu^{A/B}$ is the average number of dark counts per detector, $\xi^{A/B}$ is the average number of uncorrelated photons due to the environment, losses, and detector inefficiencies, γ is the average number of detectable correlated photons, and finally C is a related, also dimension-independent, parameter (for details, see Appendix D). We can now express the achievable key rate in bits/s as $K(d) = R(d, v) K_{\text{tot}}^{\text{iso}}(d, v, k)$. In Fig. 2, we plot $K(d)$ versus the total dimension d for different choices of subspace size k .

IV. CONCLUSIONS

We present a simultaneous subspace coding entanglement-based HD QKD protocol. Using two noise models for the most paradigmatic platforms for photonic HD entanglement, we showcase that the protocol can indeed provide a viable pathway toward practically improved QKD. Most of the improvement comes from

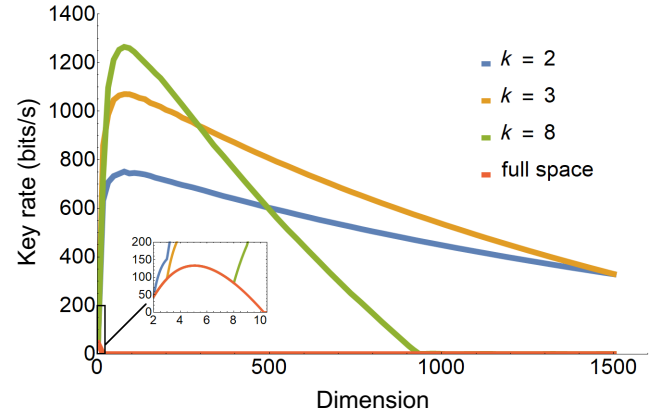


FIG. 2. The achievable key rates versus the dimension for different subspace encodings in the spatial domain. The parameters that we use here are as follows: detector efficiencies $P_C = 60\%$, losses for one party $P_L = 98.4\%$, dark counts $\mu = 600$ clicks/s, environmental photons $\nu = 21\,000$ photons/s, coincidence window $\Delta t = 10^{-7}$ s, average laser photons (at source) $\lambda = 200\,000$ photons/s. Increasing the Hilbert space by adding detectors imposes a natural limit beyond which the extra dimensions are not useful, but in fact detrimental. Also, different subspace sizes are optimal for different total dimensions. Except for small dimensions, the subspace encoding tremendously increases key rates over traditional full encoding.

the fact that encoding in subspaces of HD systems is more resilient to physical noise [56], compared to directly encoding in a comparable dimension. It seems counter-intuitive that a qubit subspace reaches the highest noise resistance, when the entire premise is that HD systems are inherently more resistant to noise. The principal reason is that for the most common experimental implementations, the entanglement of the HD state is also present in two-dimensional subspaces, where the cost of error correction is the lowest. So, while larger subspaces feature more entanglement, smaller subspaces have a smaller error correction overhead, leading to this intricate interplay between noise, rate, and subspace dimension that we observe. And in the cases of extremal noise, they are the smallest subspaces that yield the highest (or any) key. Surprisingly, the optimal subspace size in noisy scenarios often goes beyond two dimensions. The actual value of achievable key rates highly depends on the implementation and specific noise parameters, from dark counts and background to losses and device fidelities. For all parameter ranges, HD encodings lead to improved key rates. We believe that our noise models together with the semidefinite programs (SDPs) for computing key rates for our protocol will be useful for optimizing system parameters for a broad family of future setups. The security analysis and the noise models can be further refined and adjusted accordingly to account for other sources of noise and different noise regimes. For instance, at the noise regime that

we consider, multiphoton detection events are negligible; therefore, we discard them without affecting the security of the protocol. However, in different noise regimes, simply discarding these events might open up a security loophole and the security analysis should account for them, e.g., by treating them as additional noise (decreasing the key rate) depending on the implementation. Last but not least, the theoretical predictions for the achievable key rates presented in this paper have recently been successfully verified in a proof-of-principle implementation of our protocol using photons entangled in the path degree of freedom [65].

ACKNOWLEDGMENTS

We would like to thank Mateus Araújo for his comments. M.H. acknowledges funding from the Austrian Science Fund (FWF) through the START Project No. Y879-N27. C.V. acknowledges support from the Belgian Fonds de la Recherche Scientifique (FNRS), under Grant No. R.50.05.18.F (“Quantum Algorithms and Applications,” QuantAlgo). The QuantAlgo project has received funding from the QuantERA European Research Area Network (ERA-NET) Cofund in Quantum Technologies implemented within the European Union’s Horizon 2020 program. C.V. also acknowledges support from the Fundação para a Ciência e a Tecnologia (FCT) through the FCT projects “Quantum primitives for privacy preserving data mining” (QuantumMining) POCI-01-0145-FEDER-031826 and “Development of a quantum random number generator network server” (QuRUNNER) UIDB/EEA/50008/2019 supported by national funds, by the European Regional Development Fund (FEDER), through the Competitiveness and Internationalization Operational Programme (COMPETE 2020), and by the Regional Operational Program of Lisbon. G.M. is funded by the Deutsche Forschungsgemeinschaft (DFG) (the German Research Foundation) under Germany’s Excellence Strategy—Cluster of Excellence Matter and Light for Quantum Computing (ML4Q) EXC 2004/1—390534769. M.D., M.Pi., and M.Pl. acknowledge funding from Vedecká Grantová Agentúra project 2/0136/19. M.Pi. and M.Pl. additionally acknowledge Grant Agency of Masaryk University project MUNI/G/1596/2019.

APPENDIX A: KEY RATES OF THE SUBSPACE-QKD PROTOCOL

Here, we prove the key-rate expression for the subspace-QKD protocol, Protocol 1. The key rate can be computed using the key rates of each subspace, as stated in the following theorem.

Theorem 1. *The asymptotic key rate of the subspace-QKD protocol, Protocol 1, is given by*

$$K_{tot} \geq \sum_{m=0}^{\ell-1} p(M=m)[H(X'|E)_{\tilde{\rho}^m} - H(X'|Y)_{\tilde{\rho}^m}], \quad (\text{A1})$$

where the conditional entropies are evaluated on the states $\tilde{\rho}_{X'Y'E}^m$ given by

$$\tilde{\rho}_{X'Y'E}^m = (\mathcal{E}_{X'Y' \leftarrow AB}^{\mathcal{M}} \otimes id_E)(|\tilde{\psi}_{ABE}^m\rangle) \quad (\text{A2})$$

and $|\tilde{\psi}_{ABE}^m\rangle$ is the purification of the state

$$\rho_{AB}^m = \frac{\Pi_A^m \otimes \Pi_B^m(\rho_{AB})\Pi_A^m \otimes \Pi_B^m}{p(M=m)} \quad (\text{A3})$$

with

$$p(M=m) = \text{Tr}(\Pi_A^m \otimes \Pi_B^m \rho_{AB}). \quad (\text{A4})$$

Proof: The protocol explores multiple subspaces of size k , where $d = \ell \times k$. Then, both \mathcal{H}_A and \mathcal{H}_B can be divided into ℓ subspaces of size k as $\mathcal{H}_A = \mathcal{H}_{A_0} \oplus \dots \oplus \mathcal{H}_{A_{\ell-1}}$ and $\mathcal{H}_B = \mathcal{H}_{B_0} \oplus \dots \oplus \mathcal{H}_{B_{\ell-1}}$.

The QKD protocol involves two measurement settings: $\{A_1^x\}_{x=0}^{d-1}$ and $\{B_1^y\}_{y=0}^{d-1}$ denote the computational bases of \mathcal{H}_A and \mathcal{H}_B , respectively, and $\{A_2^x\}_{x=0}^{d-1}$, $\{B_2^y\}_{y=0}^{d-1}$ are sums of mutually unbiased measurements in subspaces of size k . Formally, $A_2^x = UA_1^x U^\dagger$ and $B_2^y = U^* B_1^y U^T$, where $U = \sum_{m=0}^{\ell-1} \sum_{i,j=0}^{k-1} \omega_k^{ij} |mk+i\rangle \langle mk+j|$ and $\omega_k = e^{(2\pi i/k)}$. Note that the two measurements of the parties are block diagonal with blocks of size k . Therefore, Alice’s measurement outcome $x = mk + i$ is interpreted as outcome i in the m th subspace. Bob’s measurement outcomes are interpreted analogously.

The subspace-QKD protocol, given in the main text, can be divided into the following maps:

$$\begin{aligned} \mathcal{E}_{K_A K_B E' \leftarrow ABE}^{\text{SubspaceQKD}}(\rho_{ABE}) &= \mathcal{E}_{K_A K_B E' \leftarrow X'Y'E'}^{\text{IR-PA}} \circ \mathcal{E}_{X'Y'E' \leftarrow XYE}^{\text{Sub}} \\ &\quad \circ (\mathcal{E}_{XY \leftarrow AB}^{\mathcal{M}} \otimes id_E)(\rho_{ABE}), \end{aligned} \quad (\text{A5})$$

where $\mathcal{E}_{XY \leftarrow AB}^{\mathcal{M}} \otimes id_E$ represents the measurements implemented in Step 2, $\mathcal{E}_{X'Y'E' \leftarrow XYE}^{\text{Sub}}$ corresponds to the subspace selection implemented in Step 3 and, finally, $\mathcal{E}_{K_A K_B E'}^{\text{IR-PA}}$ describes the classical postprocessing applied to the raw key consisting of information reconciliation and privacy amplification.

The difference between the subspace-QKD protocol, Protocol 1, and a standard high-dimensional QKD protocol is in the subspace selection described in Step 3. The selection of subspaces, Step 3 in Protocol 1, corresponds

to Alice and Bob applying a local projection described by $\{\Pi^m\}_{m=0}^{\ell-1}$ with elements

$$\Pi^m = \sum_{i=0}^{k-1} |mk + i\rangle\langle mk + i| \quad (\text{A6})$$

and selecting the cases where both get the same outcome. This step resembles the procedure called *advantage distillation* that has been studied in the classical setting [61] as well as in QKD protocols [62–64]. Indeed, the subspace selection in Step 3 aims to select the rounds in which higher correlations between Alice and Bob are observed. This is exactly the objective of advantage distillation procedures such as those studied in Ref. [62–64]. However, the procedures studied in Ref. [62–64] consist of processing several rounds together (corresponding to a joint quantum operations in several copies of the state) while the procedure given by Step 3 only involves one copy of the state (and corresponds to a single copy-filter operation).

Now, note that the map implemented in Step 3 is a projection into subspaces and this operation commutes with both Alice's and Bob's measurements. Therefore we can, instead, describe the QKD protocol as, first, Alice and Bob performing the projection and then proceeding with the measurements in the resulting state:

$$\begin{aligned} \mathcal{E}_{K_A K_B E' \leftarrow ABE}^{\text{SubspaceQKD}}(\rho_{ABE}) &= \mathcal{E}_{K_A K_B E' \leftarrow X' Y' E'}^{\text{IR-PA}} \circ (\mathcal{E}_{X' Y' \leftarrow A' B'}^{\mathcal{M}} \otimes id_E) \\ &\circ \mathcal{E}_{A' B' E' \leftarrow ABE}^{\text{Sub}}(\rho_{ABE}). \end{aligned} \quad (\text{A7})$$

So, in order to perform the security analysis, we will use this alternative description. Our goal is to determine the state shared by the parties after the action of the map $\mathcal{E}_{A' B' E' \leftarrow ABE}^{\text{Sub}}$. Initially, Eve distributes a state ρ_{AB} to Alice and Bob such that she holds a purification of it:

$$\rho_{AB} = \text{Tr}_E |\psi_{ABE}\rangle\langle\psi_{ABE}|. \quad (\text{A8})$$

Application of the map $\mathcal{E}_{A' B' E' \leftarrow ABE}^{\text{Sub}}(|\psi\rangle_{ABE})$ leads to

$$\mathcal{E}_{A' B' E' \leftarrow ABE}^{\text{AD}}(\rho_{ABE}) = \rho_{A' B' E M}, \quad (\text{A9})$$

where the register M records the result of the projection, i.e., M takes value m if $m_A = m_B = m$, and $M = \perp$ otherwise:

$$\begin{aligned} \rho_{A' B' E M} &= \sum_{m=0}^{\ell-1} p(M = m) \rho_{ABE}^m \otimes |m\rangle\langle m|_M \\ &+ p(M = \perp) |\perp\rangle\langle\perp| \otimes |\perp\rangle\langle\perp|_{AB} \otimes \rho_E \otimes |\perp\rangle\langle\perp|_M, \end{aligned} \quad (\text{A10})$$

where

$$\rho_{ABE}^m = \frac{\Pi_A^m \otimes \Pi_B^m \otimes I_E (|\psi_{ABE}\rangle\langle\psi_{ABE}|) \Pi_A^m \otimes \Pi_B^m \otimes I_E}{p(M = m)} \quad (\text{A11})$$

and $p(M = m)$ is the probability that Alice and Bob get outcome m in the projection, given by

$$p(M = m) = \text{Tr}(\Pi_A^m \otimes \Pi_B^m \otimes I_E |\psi_{ABE}\rangle\langle\psi_{ABE}|). \quad (\text{A12})$$

Now, Alice and Bob will perform measurements on the state given in Eq. (A10) in order to generate a key:

$$\rho_{X' Y' E M} = \mathcal{E}_{X' Y' \leftarrow A' B'}^{\mathcal{M}} \otimes id_{EM}(\rho_{A' B' E M}) \quad (\text{A13})$$

The entropy of Alice's outcome after measuring the state $\rho_{A' B' E M}$, conditioned on the information available to the eavesdropper, is given by

$$H(X'|EM)_{\rho_{X' E M}} = \sum_{m=0}^{\ell-1} p(M = m) H(X'|EM = m)_{\rho_{X' E M}} \quad (\text{A14})$$

$$= \sum_{m=0}^{\ell-1} p(M = m) H(X'|E)_{\rho_{X' E}^m} \quad (\text{A15})$$

$$\geq \sum_{m=0}^{\ell-1} p(M = m) H(X'|E)_{\tilde{\rho}_{X' E}^m}. \quad (\text{A16})$$

The first equation follows from the properties of conditional von Neumann entropy for classical-quantum states. In the last step, we consider the entropy evaluated on the state that results from Alice and Bob applying the measurements to $\tilde{\rho}_{A' B' E M}$, where

$$\begin{aligned} \tilde{\rho}_{A' B' E M} &= \sum_{m=0}^{\ell-1} p(M = m) \tilde{\rho}_{ABE}^m \otimes |m\rangle\langle m|_M \\ &+ p(M = \perp) |\perp\rangle\langle\perp| \otimes |\perp\rangle\langle\perp|_{AB} \otimes \rho_E \otimes |\perp\rangle\langle\perp|_M \end{aligned} \quad (\text{A17})$$

and

$$\tilde{\rho}_{ABE}^m = \text{Tr}_E |\psi_{ABE}^m\rangle\langle\psi_{ABE}^m|, \quad (\text{A18})$$

where $|\psi_{ABE}^m\rangle$ is the purification of ρ_{AB}^m . Giving Eve the purification of ρ_{AB}^m before the measurements only increases her power, which proves the lower bound. Similarly, for the required information to be exchanged for information reconciliation,

$$H(X'|Y' M)_{\rho_{X' Y' M}} = \sum_{m=0}^{\ell-1} p(M = m) H(X'|Y' M = m)_{\rho_{X' Y' M}} \quad (\text{A19})$$

$$= \sum_{m=0}^{\ell-1} p(M = m) H(X'|Y')_{\rho_{X' Y'}^m} \quad (\text{A20})$$

$$= \sum_{m=0}^{\ell-1} p(M = m) H(X'|Y')_{\tilde{\rho}_{X' Y'}^m} \quad (\text{A21})$$

and the last step follows from the fact that $\tilde{\rho}_{AB}^m = \rho_{AB}^m$. ■

APPENDIX B: SOLUTION OF THE SDP AND THE CHOICE OF W

In this appendix, we present in detail the optimization problem for calculating the average guessing probability of Eve and its solution. The average guessing probability is obtained by maximizing, over all possible tripartite states ρ_{ABE} (recall that Eve holds a purification of ρ_{ABE}) and all possible measurements of Eve $\{E^e\}_e$, the probability P_g that Eve guesses Alice's outcomes and then performing a weighted average of these probabilities:

$$P_g = \max_{\rho_{ABE}, \{E^e\}_{e=0}^{d-1}} \sum_{e,y} \text{Tr}(\rho_{ABE} A_1^e \otimes B_1^y \otimes E^e)$$

such that $\text{Tr}(\widehat{W}\rho_{AB}) = W$,

$$\begin{aligned} \rho_{ABE} &\geq 0, \\ \text{Tr}(\rho_{ABE}) &= 1, \\ E^e &\geq 0 \forall e, \\ \sum_e E^e &= \mathbb{1}, \end{aligned} \quad (\text{B1})$$

where A_1 and B_1 stand for the computational basis and \widehat{W} is the yet-to-be-defined operator, with W its measured value that constrains the optimization. W will be constructed depending on which *target* state the experiment is trying to produce. Here, we consider W to be the average value of equal outcomes that Alice and Bob get in the second basis, $W = \sum_x P(xx|22)$, which is the average value of the operator $\widehat{W} = \sum_x A_2^x \otimes B_2^x$. Our goal now is to express the guessing probability as a function of W and d , by solving the following optimization problem, which we obtain from the previous one by substituting $\rho_e := \text{Tr}_E(\rho_{ABE} E^e)$:

$$P_g(W, d) = \max_{\{\rho_e\}_e} \sum_{e=0}^{d-1} \text{Tr}(\rho_e A_1^e \otimes \mathbb{1}_d)$$

such that $\text{Tr}\left(\widehat{W} \sum_{e=0}^{d-1} \rho_e\right) = W$,

$$\begin{aligned} \rho_e &\geq 0, \forall e \in \{0, \dots, d-1\}, \\ \text{Tr}\left(\sum_{e=0}^{d-1} \rho_e\right) &= 1, \end{aligned}$$

the dual of which is

$$\begin{aligned} \min_{\gamma, S} \gamma + SW, \\ \text{such that } \gamma \mathbb{1}_{d^2} + S\widehat{W} &\geq |e\rangle\langle e| \otimes \mathbb{1}_d, \forall e. \end{aligned}$$

The nonzero eigenvalues of $S\widehat{W} - |e\rangle\langle e| \otimes \mathbb{1}_d$, as a function of S and the local dimension d , for a given

e are $\lambda_{\pm} = [S - 1 \pm \sqrt{(S-1)^2 + 4S(d-1)/d}/2]$ (each one with degeneracy d) and the optimization now reads

$$\begin{aligned} \min_{\gamma, S} \gamma + SW, \\ \text{such that } \gamma + \lambda_{-} &\geq 0 \forall e, \\ \gamma + \lambda_{+} &\geq 0 \forall e. \end{aligned}$$

Since $\lambda_{+} \geq \lambda_{-}$, for all S, d , and λ_{\pm} are the same for all e , we can relax the constraints to

$$\begin{aligned} \min_{\gamma, S} \gamma + SW, \\ \text{such that } \gamma + \lambda_{-} &\geq 0. \end{aligned}$$

We finally solve $(\partial/\partial S)\lambda_{-} = W$, which gives

$$\begin{aligned} W &= \frac{1}{2} \left(1 - \frac{2S + 2 - 4/d}{2\sqrt{(S-1)^2 + 4S(d-1)/d}} \right), \\ S &= \frac{2}{d} - 1 + \frac{1 - 2W}{d} \sqrt{\frac{d-1}{W(1-W)}} \text{ and} \\ \lambda_{-} &= -\frac{d-1}{d} - \frac{W}{d} \sqrt{\frac{d-1}{W(1-W)}}, \end{aligned}$$

and obtain the form of the guessing probability as a function of W and d :

$$P_g(W, d) = -\lambda_{-} + SW = \frac{(\sqrt{W} + \sqrt{(d-1)(1-W)})^2}{d}.$$

APPENDIX C: IMPLEMENTATION WITH TEMPORAL DEGREES OF FREEDOM

We start by considering a hyperentangled state of the form

$$|\Psi\rangle = |\phi^{-}\rangle_{AB} \otimes \int dt f(t) |t\rangle_A \otimes |t\rangle_B. \quad (\text{C1})$$

This is the state of two entangled photons (one for Alice and one for Bob), with two degrees of freedom: the time of arrival t of the photons at Alice's and Bob's respective laboratories and their polarization. The time of arrival, i.e., the time at which the detector clicks, is a continuous variable, which can be discretized by considering time bins of size t_b . Setting a time frame F outside of which a photon is "lost" and taking F to be a multiple of t_b , we effectively have a discrete system of dimension $d = (F/t_b)$.

The probability that at the frame $[0, F]$ exactly n pairs of entangled photons are produced is given by the Poisson

distribution:

$$P_F(n) = \frac{(\lambda F)^n e^{-\lambda F}}{n!},$$

where λ is the production rate of the photon pairs. Both F and λ are tunable parameters and we assume that λ is small enough such that multiphoton events in the same frame are negligible. In particular, we choose λ such that

$$\begin{aligned} P_F(n \geq 2) &= 1 - P_F(0) - P_F(1) \\ &= 1 - (1 + \lambda F)e^{-\lambda F} < \epsilon. \end{aligned}$$

The average number of photons per frame is λF and for $\lambda F < 0.2$ we obtain $P_F(n \geq 2) < 0.015$, which is small enough with respect to the noise scale in our model. Note, though, that by decreasing the production rate λ we are also decreasing the key rate [see Eq. (C3) at the end of this section]; therefore, we should tune these parameters carefully.

We consider two types of noise, namely the noise due to the interaction of the photons with the environment before entering Alice's and Bob's laboratories and the noise introduced due to the detector inefficiency. Because of its interaction with the environment, a photon can be lost with probability P_L . Given n photons, the probability that n_L of them are lost while the rest arrive at the laboratory is $P_L^{n_L} (1 - P_L)^{n - n_L} \binom{n}{n_L}$.

Moreover, photons from the environment may be introduced in the system. We assume that the environment produces, on average, ν photons per second. The number of photons arriving within the frame from the environment will then follow the Poisson distribution, $P_E(n) = (\nu F)^n e^{-\nu F} / (n!)$.

As far as the noise due to the detectors is concerned, each detector has probability P_C of clicking when a photon arrives and probability per second μ of clicking when no photon is present. These events are called dark counts and they also follow the Poisson distribution, $P_D(n) = (\mu F)^n e^{-\mu F} / (n!)$.

The probability that both Alice and Bob receive (i, j) photons in their laboratories in a time frame F is

$$\begin{aligned} P(i, j) &= \sum_{n=0}^{\infty} \sum_{n_1=\max\{n-i, 0\}}^n \sum_{n_2=\max\{n-j, 0\}}^n P_F(n) \\ &\quad \times P_L^{n_1} (1 - P_L)^{n - n_1} \binom{n}{n_1} P_L^{n_2} (1 - P_L)^{n - n_2} \binom{n}{n_2} \\ &\quad P_E(i - n + n_1) P_E(j - n + n_2). \end{aligned}$$

Given that i photons enter, the probability of obtaining exactly one click in a frame F is

$$\begin{aligned} P(\text{click}|i) &= (1 - P_C)^{i-1} [P_C P_D(0) i + (1 - P_C) P_D(1)] \\ &= e^{-\mu F} (1 - P_C)^i \left(\frac{i P_C}{1 - P_C} + \mu F \right), \end{aligned}$$

and the probability that both Alice and Bob obtain one click is $P(11) = \sum_{i,j=0}^{\infty} P(\text{click}|i) P(\text{click}|j) P(i, j)$.

After applying the approximation $P_F(n \geq 2) \approx 0$, we can calculate $P(11)$ to be

$$P(11) \approx e^{-F[2(\mu + \nu P_C) + \lambda]} F \beta,$$

where $\beta := [\lambda \alpha^2 + F(\mu + \nu P_C)^2]$ and $\alpha := [P_C(1 - P_L) + F(\mu + P_C \nu) P_L + F(\mu + \nu P_C)(1 - P_C)(1 - P_L)]$.

In the above expressions note that, if only a photon pair is produced, the probability that it passes and gets detected is $P_C(1 - P_L)$, the probability that it passes but does not get detected is $(1 - P_C)(1 - P_L)$, and the probability that it gets lost is P_L , and an environmental photon or a dark count is making the click instead, with probability $[F(\mu + \nu P_C)]$. The term $e^{-2(\mu + \nu P_C)F}$ is the probability that all the extra photons of the environment are not detected and there are no dark counts. If there is no pair in the frame, the click must have come from the environment or it is a dark count.

If the setup is asymmetric (one detector is close to the source, the other is far away), we can modify the formula to include different parameters for Alice and Bob:

$$\begin{aligned} P(11) &\approx e^{-(\mu^A + \mu^B + \nu^A P_C^A + \nu^B P_C^B + \lambda)F} \\ &\quad \times \left[\lambda \alpha^A \alpha^B + F(\mu^A + \nu^A P_C^A)(\mu^B + \nu^B P_C^B) \right]. \end{aligned}$$

In our noise model, we do not consider finite-size effects (the number of rounds is sufficiently large) and neither border effects on the frame (F is sufficiently large, so the error of the clock that decides when the frame begins and ends is negligible) nor errors related to the relaxation time of the detectors (which is the time a detector needs before being able to detect another photon—if the frame was approximately the same size as the relaxation time, this effect would be important, but we choose F to be sufficiently large for this purpose). We also assume that the interaction with the environment can only destroy a photon and that the photon pairs coming from the environment are uncorrelated. Furthermore, F and the production rate λ are chosen such that the probability of observing two or more entangled photons during a single frame is negligible. With these assumptions, we have a model that gives us the rate of “valid” rounds per second, as a function of F , which, in turn, is proportional to the local dimension d :

$$R(d) = P(11)/F = e^{-F[2(\mu + \nu P_C) + \lambda]} \beta. \quad (\text{C2})$$

For large $F = dt_b$, we have $\beta \approx F(\mu + \nu P_C)^2 [(1 + P_C P_L - P_C)^2 + \lambda F] \propto F$.

We can also estimate the visibility, i.e., the probability that—given that both parties have exactly one click—the photons that click are the entangled ones coming from the laser source and not the environment or dark counts. First,

we calculate the probability that a photon pair will survive and get detected,

$$P_S = P_F(1)(1 - P_L)^2 P_C^2 e^{-2F(\mu + \nu P_C)},$$

which gives the visibility as a function of the dimension d to be $v(d) = P_S/P(11) = \lambda(1 - P_L)^2 P_C^2 / \beta$, while for an asymmetric setup we have $v(d) = \lambda(1 - P_L^A)(1 - P_L^B) P_C^A P_C^B / \beta$.

Finally, for large d , $\lambda \propto 1/F$ and $\beta \propto F$, thus making the visibility scale as d^{-2} .

In order to take multiphoton events into account, we write α and $P(11)$ as

$$\alpha(n) = (1 - P_C + P_C P_L)^{n-1} [n P_C (1 - P_L) + F(\mu + \nu P_C)(1 - P_C + P_C P_L)],$$

$$P(11) = e^{-(\mu^A + \mu^B + \nu^A P_C^A + \nu^B P_C^B)F} \sum_{n=0}^{\infty} P_F(n) \alpha^A(n) \alpha^B(n)$$

and obtain

$$P(11) = e^{-F(T_A + T_B + \gamma)} (F^2 T_A T_b + F\gamma) \quad \text{and} \\ R = e^{-F(T_A + T_B + \gamma)} (F T_A T_b + \gamma), \quad (C3)$$

where $S = 1 - P_C + P_C P_L$, $Q = \mu + \nu P_C$, $T_{A/B} = Q^{A/B} + \lambda S^{B/A}(1 - S^{A/B})$ and $\gamma = \lambda(1 - S^A)(1 - S^B)$.

Accordingly, the generalized success probability becomes

$$P_S = e^{-F(Q^A + Q^B)} \sum_{n=0}^{\infty} P_F(n) (S^A S^B)^{n-1} (1 - S^A)(1 - S^B) n \\ = e^{-F(T_A + T_B + \gamma)} \gamma F.$$

The maximum of P_S is for $F = 1/(T_A + T_B + \gamma)$ and the visibility becomes $v = 1/(1 + F T_A T_B \gamma^{-1})$.

APPENDIX D: IMPLEMENTATION WITH SPATIAL DEGREES OF FREEDOM

A basic parameter of our model is Δt , the coincidence window in which two events, for Alice and Bob, are considered coincident. Note that multiple clicks in the same coincidence window are treated as a single event. Another parameter is related to the projection of an infinite-dimensional entangled state of the form $|\Psi\rangle = \sum_{l=-\infty}^{\infty} c_l |l\rangle_A \otimes |-l\rangle_B$ into a finite dimensional space. This is the probability $P_P(d) := \text{Tr}(\mathbb{1}_{d^2} |\Psi\rangle\langle\Psi| \mathbb{1}_{d^2})$, which we assume to be constant, thus providing lower dimensions with an advantage. One could give an advantage to higher dimensions by dropping this assumption.

In our model Fig. 3, we consider that a click can come either from the laser or from the environment or from the dark counts. We start with the laser photons, by assuming that they follow a Poisson distribution, factorized by the probability $P_P(d)$ of being within the modes $-d/2$ and $d/2$. The probability that the laser produces j detectable photons given that n in total are emitted is $(\Delta t \lambda)^n (e^{-\Delta t \lambda} / n!) P_P^j(d) [1 - P_P(d)]^{n-j} \binom{n}{j}$.

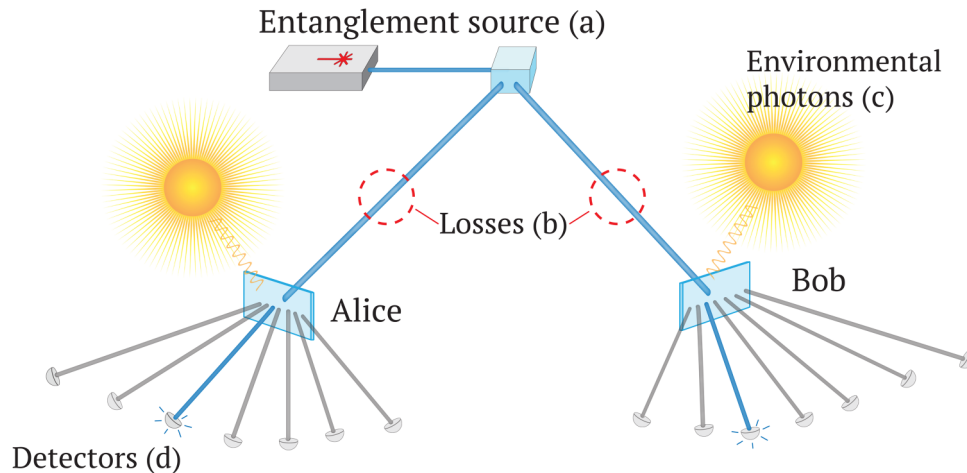


FIG. 3. A schematic representation of the noise model: a laser source (a) produces entangled pairs distributed in time with a Poisson distribution, with λ as the average number of photons per second. The pairs are distributed to the parties and suffer from party-dependent losses (b) with probability P_L . On top of the entangled photons, the parties receive ν environmental photons (c) per second on average, distributed as well with a Poissonian. For each of the modes that are being measured, there is an associated detector (d), which comes with an average number of dark counts μ per second and an efficiency P_C .

Given j photons produced from the laser, the probability they produce no click in one of the laboratories is

$$P(0|j) = \sum_{r=0}^j P_L^{j-r} (1 - P_L)^r \binom{j}{r} (1 - P_C)^r \binom{r}{0} = [1 - P_C(1 - P_L)]^j = (1 - T)^j, \text{ where } T = P_C(1 - P_L),$$

while the probability that they produce one or more clicks in a single detector is

$$\begin{aligned} P(1|j) &= \sum_{r_1=1}^j P_L^{j-r_1} (1 - P_L)^{r_1} \binom{j}{r_1} \sum_{r_2=1}^{r_1} \left(\frac{d-1}{d}\right)^{r_1-r_2} (1 - P_C)^{r_1-r_2} \left(\frac{1}{d}\right)^{r_2} [1 - (1 - P_C)^{r_2}] \binom{d}{1} \binom{r_2}{r_1} \\ &= d \left[(1 - T + \frac{T}{d})^j - (1 - T)^j \right]. \end{aligned}$$

In the above, P_L reflects the losses affecting the entangled photons, and we further assume that all modes suffer the same losses; therefore, we absorb them in P_C . In the case in which one would like to further refine the noise model, different losses for different modes could be taken into consideration. We also calculate the probability that, given j photons are produced, Alice and Bob both get one click from a laser photon in different detectors, as in this way we account for entangled photons. We have

$$\begin{aligned} P(\neq|j) &= d(d-1) \sum_{\substack{r_1, r_2, r_3=0 \\ r_0+r_1+r_2+r_3=j}}^j \sum_{r_0=0}^{j-1} \frac{j!}{r_0!r_1!r_2!r_3!} \times (P_L^A P_L^B)^{r_0} [P_L^B(1 - P_L^A)]^{r_1} [P_L^A(1 - P_L^B)]^{r_2} [(1 - P_L^A)(1 - P_L^B)]^{r_3} \\ &\times \sum_{l_1=0}^{r_1} \left(\frac{d-1}{d}\right)^{r_1-l_1} (1 - P_C^A)^{r_1-l_1} \binom{1}{d}^{l_1} \binom{r_1}{l_1} \times \sum_{l_2=0}^{r_2} \left(\frac{d-1}{d}\right)^{r_2-l_2} (1 - P_C^B)^{r_2-l_2} \binom{1}{d}^{l_2} \binom{r_2}{l_2} \\ &\times \sum_{\substack{s_3, p_3, q_3=0 \\ s_3+p_3+q_3=r_3}}^{r_3} \left(\frac{1}{d}\right)^{s_3+p_3} \left(\frac{d-2}{d}\right)^{q_3} \frac{r_3!}{s_3!p_3!q_3!} (1 - P_C^B)^{s_3+q_3} (1 - P_C^A)^{p_3+q_3} \\ &\times [1 - (1 - P_C^A)^{l_1+s_3}] [1 - (1 - P_C^B)^{l_2+p_3}] \\ &= d(d-1) \left\{ [(1 - T^A)(1 - T^B)]^j + \left[(1 - T^A)(1 - T^B) + \frac{1}{d} [T^A(1 - T^B) + T^B(1 - T^A)] \right]^j \right. \\ &\quad \left. - \left[(1 - T^B)(1 - T^A + T^A/d) \right]^j - \left[(1 - T^A)(1 - T^B + T^B/d) \right]^j \right\}. \end{aligned}$$

Similarly, the probability that, given j photons, Alice and Bob both get one click from a laser photon in the same detector is

$$\begin{aligned} P(=|j) &= d \sum_{\substack{r_1, r_2, r_3=0 \\ r_0+r_1+r_2+r_3=j}}^j \sum_{r_0=0}^{j-1} \frac{j!}{r_0!r_1!r_2!r_3!} \times (P_L^A P_L^B)^{r_0} [P_L^B(1 - P_L^A)]^{r_1} [P_L^A(1 - P_L^B)]^{r_2} [(1 - P_L^A)(1 - P_L^B)]^{r_3} \\ &\times \sum_{l_1=0}^{r_1} \left(\frac{d-1}{d}\right)^{r_1-l_1} (1 - P_C^A)^{r_1-l_1} \binom{1}{d}^{l_1} \binom{r_1}{l_1} \times \sum_{l_2=0}^{r_2} \left(\frac{d-1}{d}\right)^{r_2-l_2} (1 - P_C^B)^{r_2-l_2} \binom{1}{d}^{l_2} \binom{r_2}{l_2} \end{aligned}$$

$$\begin{aligned}
& \times \sum_{l_3=0}^{r_3} \left(\frac{d-1}{d}\right)^{r_3-l_3} \left(\frac{1}{d}\right)^{l_3} (1-P_C^B)^{r_3-l_3} (1-P_C^A)^{r_3-l_3} \binom{r_3}{l_3} \times [1 - (1-P_C^A)^{l_1+l_3}] [1 - (1-P_C^B)^{l_2+l_3}] \\
& = d \left\{ [(1-T^A)(1-T^B)]^j + \left[(1-T^A)(1-T^B) + \frac{1}{d} [T^A(1-T^B) + T^B(1-T^A) + T^A T^B] \right]^j \right. \\
& \quad \left. - \left[(1-T^A + T^A/d)(1-T^B) \right]^j - \left[(1-T^A)(1-T^B + T^B/d) \right]^j \right\},
\end{aligned}$$

We can now proceed to the clicks due to dark counts. Again, their distribution is Poissonian, with multiple clicks in the same detector counting as one. Therefore, the probability of no clicks in a single detector is $e^{-\Delta t \mu}$, while the probability of one or more clicks in one detector is $1 - e^{-\Delta t \mu}$. In total, the probability of n dark counts in all d detectors is $P_D(n, d) = (e^{-\Delta t \mu})^{d-n} (1 - e^{-\Delta t \mu})^n \binom{d}{n}$, which also gives another quantity that we need: the probability that, given that a detector already clicked because of a laser photon, all other detectors do not click because of dark counts. Denoting this probability by $P(0, d-1)$, we have

$$P(0, d-1) = P_D(1, d) \frac{1}{d} + P_D(0, d) = e^{-(d-1)\Delta t \mu}.$$

Finally, we consider the last type of clicks that Alice and Bob register, the ones coming from environmental photons. We assume that they are produced according to a Poisson distribution. Given r photons in the same mode, the probability that at least one of them clicks is $1 - (1 - P_C)^r$. Furthermore, the probability that r out of q photons go in the same mode, one of them clicks, while all the others do not click is

$$\sum_{r=1}^q \left(\frac{d-1}{d}\right)^{q-r} (1-P_C)^{q-r} \left(\frac{1}{d}\right)^r [1 - (1-P_C)^r] \binom{q}{r} = \left[1 - \frac{P_C(d-1)}{d}\right]^q - (1-P_C)^q$$

and we multiply it with the Poissonian distribution of environmental photons and the number of modes to obtain

$$\begin{aligned}
P_E(1, d) &= d \sum_{q=0}^{\infty} (\nu \Delta t)^q \left[1 - \frac{P_C(d-1)}{d}\right]^q \frac{e^{-\nu \Delta t}}{q!} - d \sum_{q=0}^{\infty} (\nu \Delta t)^q (1-P_C)^q \frac{e^{-\nu \Delta t}}{q!} \\
&= d P_E(0^*, d) (1 - e^{-P_C \nu \Delta t / d}),
\end{aligned}$$

with $P_E(0^*, d) = e^{-P_C \nu \Delta t (d-1)/d}$, which is the probability that, in the case in which a detector already clicked because of a laser photon or a dark count, r out of q environmental photons end up in this detector, while the remaining $q-r$ end up in the other detectors and none of them clicks. Note that losses affecting environmental photons are absorbed in ν .

With all the above in place, we can now calculate the quantities of interest, namely the visibility and the key rate. We start with the probability that, given j photons locally, a single detector clicks,

$$\begin{aligned}
P(1) &= P(1|j) P_D(0, d-1) P_E(0^*, d) + P(0|j) P_D(1, d) P_E(0^*, d) + P(0|j) P_D(0, d) P_E(1, d) \\
&= d P_D(0, d-1) P_E(0^*, d) \left[\left(1 - T + \frac{T}{d}\right)^j - (1 - T)^j e^{-\Delta t (\mu + P_C \nu / d)} \right],
\end{aligned}$$

and we continue with the probability that both parties get a single click,

$$\begin{aligned}
P(11) &= \sum_{n=0}^{\infty} \sum_{j=0}^n (\Delta t \lambda)^n \frac{e^{-\Delta t \lambda}}{n!} P_P^j(d) [1 - P_P(d)]^{n-j} \binom{n}{j} \\
& \times \{ [P(1|j) P_D(0, d-1) P_E(0^*, d) + P(0|n) P_D(1, d) P_E(0^*, d) + P(0|n) P_D(0, d) P_E(1, d)]^A \\
& \times [P(1|j) P_D(0, d-1) P_E(0^*, d) + P(0|n) P_D(1, d) P_E(0^*, d) + P(0|n) P_D(0, d) P_E(1, d)]^B \\
& + [P_D(0, d-1) P_E(0^*, d)]^A [P_D(0, d-1) P_E(0^*, d)]^B [P(\neq |j) + P(= |j) - P^A(1|j) P^B(1|j)] \} \\
& = d e^{-\Delta t (d-1) (\mu^A + \xi^A / d + \mu^B + \xi^B / d)} e^{-\Delta t \gamma} \left\{ d \left(1 - e^{-\Delta t (\mu^A + \xi^A / d)}\right) \left(1 - e^{-\Delta t (\mu^B + \xi^B / d)}\right) + e^{\Delta t \gamma / d} - 1 \right\},
\end{aligned}$$

where

$$\xi^{A/B} = P_C^{A/B} v^{A/B} + P_P(d) \lambda P_C^{B/A} (1 - P_L^{B/A}) (1 - P_C^{A/B} + P_C^{A/B} P_L^{A/B}) \text{ and}$$

are all experimental constants independent of d . Note that γ is the same as in the previous implementation of temporal encoding and represents the average number of detectable entangled photons, while ξ represents the environmental and laser photons that click independently in the laboratories. We are now able to write that the rate of “valid” rounds per second is

$$R(d) = \frac{P(11)}{\Delta t} = C e^{-d(\mu^A + \mu^B)} e^{(\xi^A + \xi^B)/d} \left\{ d^2 \left[1 - e^{-(\mu^A + \xi^A/d)} \right] \left[1 - e^{-(\mu^B + \xi^B/d)} \right] + d (e^{\gamma/d} - 1) \right\},$$

where $C = e^{\Delta t(\mu^A + \mu^B - \xi^B - \xi^B - \gamma)} / \Delta t$.

Finally, in order to obtain the expression for the visibility, we need the probability that an entangled pair clicks at both laboratories, while all other detectors do not click. However, once the detectors click because of the entangled pair, they might also receive any number of other photons and register dark counts. We can work around this cumbersome calculation by directly considering the probability that the same detector clicks for both Alice and Bob (which is due to the correlated photons and the noise) and subtracting the probability that different detectors click (which is due to the noise only). Essentially, we subtract the $P(\neq |j)$ contribution in $P(11)$ from its $P(= |j)$ contribution to obtain

$$P_S = d e^{-\Delta t(d-1)(\mu^A + \xi^A/d + \mu^B + \xi^B/d)} e^{-\Delta t \gamma} (e^{\Delta t \gamma/d} - 1),$$

which, in turn, gives us the visibility

$$v(d) = \frac{P_S}{P(11)} = \frac{1}{1 + d (1 - e^{-\Delta t(\mu^A + \xi^A/d)}) (1 - e^{-\Delta t(\mu^B + \xi^B/d)}) (e^{\Delta t \gamma/d} - 1)^{-1}}.$$

By rescaling with Δt , we can also write

$$v(d) = \frac{e^{\gamma/d} - 1}{e^{\gamma/d} - 1 + d \left[1 - e^{-(\mu^A + \xi^A/d)} \right] \left[1 - e^{-(\mu^B + \xi^B/d)} \right]}.$$

Note that for large d and small Δt , the visibility scales as $v(d) \approx (1/1 + d^2 \Delta t \mu^A \mu^B \gamma^{-1})$.

[1] C. H. Bennett and G. Brassard, Quantum cryptography: Public key distribution and coin tossing, *Theor. Comput. Sci.* **560**, 7 (2014), [theoretical Aspects of Quantum Cryptography—celebrating 30 years of BB84](#).

[2] A. K. Ekert, Quantum Cryptography Based on Bell’s Theorem, *Phys. Rev. Lett.* **67**, 661 (1991).

[3] V. Scarani, H. Bechmann-Pasquinucci, N. J. Cerf, M. Dušek, N. Lütkenhaus, and M. Peev, The security of practical quantum key distribution, *Rev. Mod. Phys.* **81**, 1301 (2009).

[4] H.-K. Lo, M. Curty, and K. Tamaki, Secure quantum key distribution, *Nat. Photonics* **8**, 595 (2014).

[5] S. Pirandola, U. L. Andersen, L. Banchi, M. Berta, D. Bunandar, R. Colbeck, D. Englund, T. Gehring, C. Lupo, C. Ottaviani, J. Pereira, M. Razavi, J. S. Shaari, M. Tomamichel, V. C. Usenko, G. Vallone, P. Villoresi, and P. Wallden, Advances in Quantum Cryptography, *Adv. Opt. Photonics* **12**, 1012 (2020).

[6] R. Bedington, J. M. Arrazola, and A. Ling, Progress in satellite quantum key distribution, *Npj Quantum Inf.* **3**, 30 (2017).

[7] J. G. Rarity and P. R. Tapster, Experimental Violation of Bell’s Inequality Based on Phase and Momentum, *Phys. Rev. Lett.* **64**, 2495 (1990).

[8] G. Molina-Terriza, J. P. Torres, and L. Torner, Management of the Angular Momentum of Light: Preparation of Photons in Multidimensional Vector States of Angular Momentum, *Phys. Rev. Lett.* **88**, 013601 (2001).

[9] C. H. Monken, P. H. S. Ribeiro, and S. Pádua, Transfer of angular spectrum and image formation in spontaneous parametric down-conversion, *Phys. Rev. A* **57**, 3123 (1998).

[10] G. Molina-Terriza, J. P. Torres, and L. Torner, Twisted photons, *Nat. Phys.* **3**, 305 (2007).

[11] L. Neves, G. Lima, J. G. Aguirre Gómez, C. H. Monken, C. Saavedra, and S. Pádua, Generation of Entangled States of Qudits Using Twin Photons, *Phys. Rev. Lett.* **94**, 100501 (2005).

- [12] S. Walborn, C. Monken, S. Pádua, and P. Souto Ribeiro, Spatial correlations in parametric down-conversion, *Phys. Rep.* **495**, 87 (2010).
- [13] G. Lima, L. Neves, R. Guzmán, E. S. Gómez, W. A. T. Nogueira, A. Delgado, A. Vargas, and C. Saavedra, Experimental quantum tomography of photonic qudits via mutually unbiased basis, *Opt. Express* **19**, 3542 (2011).
- [14] E. Karimi, S. A. Schulz, I. De Leon, H. Qassim, J. Upham, and R. W. Boyd, Generating optical orbital angular momentum at visible wavelengths using a plasmonic metasurface, *Light: Sci. Appl.* **3**, e167 (2014).
- [15] H. Rubinsztein-Dunlop *et al.*, Roadmap on structured light, *J. Opt.* **19**, 013001 (2016).
- [16] D. Llewellyn, Y. Ding, I. I. Faruque, S. Paesani, D. Bacco, R. Santagati, Y.-J. Qian, Y. Li, Y.-F. Xiao, and M. Huber *et al.*, Chip-to-chip quantum teleportation and multi-photon entanglement in silicon, *Nat. Phys.* **16**, 148 (2019).
- [17] J. Bavaresco, N. Herrera Valencia, C. Klöckl, M. Pivoluska, P. Erker, N. Friis, M. Malik, and M. Huber, Measurements in two bases are sufficient for certifying high-dimensional entanglement, *Nat. Phys.* **14**, 1032 (2018).
- [18] C. Schaeff, R. Polster, M. Huber, S. Ramelow, and A. Zeilinger, Experimental access to higher-dimensional entangled quantum systems using integrated optics, *Optica* **2**, 523 (2015).
- [19] J. Schneeloch, C. C. Tison, M. L. Fanto, P. M. Alsing, and G. A. Howland, Quantifying entanglement in a 68-billion-dimensional quantum state space, *Nat. Commun.* **10**, 1 (2019).
- [20] N. Herrera Valencia, V. Srivastav, M. Pivoluska, M. Huber, N. Friis, W. McCutcheon, and M. Malik, High-Dimensional Pixel Entanglement: Efficient Generation and Certification, *Quantum* **4**, 376 (2020).
- [21] E. S. Gómez, S. Gómez, I. Machuca, A. Cabello, S. Pádua, S. P. Walborn, and G. Lima, Multi-dimensional entanglement generation with multi-core optical fibers., arXiv: Quantum Physics (2020).
- [22] X.-M. Hu, W.-B. Xing, B.-H. Liu, Y.-F. Huang, C.-F. Li, G.-C. Guo, P. Erker, and M. Huber, Efficient Generation of High-Dimensional Entanglement through Multipath Down-Conversion, *Phys. Rev. Lett.* **125**, 090503 (2020).
- [23] C. Bernhard, B. Bessire, T. Feurer, and A. Stefanov, Shaping frequency-entangled qudits, *Phys. Rev. A* **88**, 032322 (2013).
- [24] S. Ramelow, L. Ratschbacher, A. Fedrizzi, N. K. Langford, and A. Zeilinger, Discrete Tunable Color Entanglement, *Phys. Rev. Lett.* **103**, 253601 (2009).
- [25] P. G. Kwiat, Hyper-entangled states, *J. Mod. Opt.* **44**, 2173 (1997).
- [26] J. T. Barreiro, N. K. Langford, N. A. Peters, and P. G. Kwiat, Generation of Hyperentangled Photon Pairs, *Phys. Rev. Lett.* **95**, 260501 (2005).
- [27] P. Vergyris, F. Mazeas, E. Gouzien, L. Labonté, O. Alibart, S. Tanzilli, and F. Kaiser, Fibre based hyperentanglement generation for dense wavelength division multiplexing, *Quantum Sci. Technol.* **4**, 045007 (2019).
- [28] P. Imany, J. A. Jaramillo-Villegas, M. S. Alshaykh, J. M. Lukens, O. D. Odele, A. J. Moore, D. E. Leaird, M. Qi, and A. M. Weiner, High-dimensional optical quantum logic in large operational spaces, *Npj Quantum Inf.* **5**, 59 (2019).
- [29] Y. Chen, S. Ecker, J. Bavaresco, T. Scheidl, L. Chen, F. Steinlechner, M. Huber, and R. Ursin, Verification of high-dimensional entanglement generated in quantum interference, *Phys. Rev. A* **101**, 032302 (2020).
- [30] A. Acin, N. Gisin, and V. Scarani, Security bounds in quantum cryptography using d -level systems, *Quantum Info. Comput.* **3**, 563 (2003).
- [31] L. Sheridan and V. Scarani, Security proof for quantum key distribution using qudit systems, *Phys. Rev. A* **82**, 030301 (2010).
- [32] M. Huber and M. Pawłowski, Weak randomness in device-independent quantum key distribution and the advantage of using high-dimensional entanglement, *Phys. Rev. A* **88**, 032309 (2013).
- [33] T. Brougham, S. M. Barnett, K. T. McCusker, P. G. Kwiat, and D. J. Gauthier, Security of high-dimensional quantum key distribution protocols using Franson interferometers, *J. Phys. B: At. Mol. Opt. Phys.* **46**, 104010 (2013).
- [34] M. Mirhosseini, O. S. Magaña-Loaiza, M. N. O'Sullivan, B. Rodenburg, M. Malik, M. P. J. Lavery, M. J. Padgett, D. J. Gauthier, and R. W. Boyd, High-dimensional quantum cryptography with twisted light, *New J. Phys.* **17**, 033033 (2015).
- [35] Y. Ding, D. Bacco, K. Dalgaard, X. Cai, X. Zhou, K. Rot-twitz, and L. K. Oxenløwe, High-dimensional quantum key distribution based on multicore fiber using silicon photonic integrated circuits, *Npj Quantum Inf.* **3**, 25 (2017).
- [36] J. Mower, Z. Zhang, P. Desjardins, C. Lee, J. H. Shapiro, and D. Englund, High-dimensional quantum key distribution using dispersive optics, *Phys. Rev. A* **87**, 062322 (2013).
- [37] C. Lee, J. Mower, Z. Zhang, J. H. Shapiro, and D. Englund, Finite-key analysis of high-dimensional time-energy entanglement-based quantum key distribution, *Quantum Inf. Process.* **14**, 1005 (2015).
- [38] D. Bunandar, Z. Zhang, J. H. Shapiro, and D. R. Englund, Practical high-dimensional quantum key distribution with decoy states, *Phys. Rev. A* **91**, 022336 (2015).
- [39] C. Lee, D. Bunandar, Z. Zhang, G. R. Steinbrecher, P. Ben Dixon, F. N. C. Wong, J. H. Shapiro, S. A. Hamilton, and D. Englund, High-rate field demonstration of large-alphabet quantum key distribution, arXiv e-prints, arXiv:1611.01139 (2016).
- [40] G. M. Nikolopoulos and G. Alber, Security bound of two-basis quantum-key-distribution protocols using qudits, *Phys. Rev. A* **72**, 032320 (2005).
- [41] G. M. Nikolopoulos, K. S. Ranade, and G. Alber, Error tolerance of two-basis quantum-key-distribution protocols using qudits and two-way classical communication, *Phys. Rev. A* **73**, 032325 (2006).
- [42] C. Vlachou, W. Krawec, P. Mateus, N. Paunković, and A. Souto, Quantum key distribution with quantum walks, *Quantum Inf. Process.* **17**, 288 (2018).
- [43] H. F. Chau, Quantum key distribution using qudits that each encode one bit of raw key, *Phys. Rev. A* **92**, 062324 (2015).
- [44] H. F. Chau, Q. Wang, and C. Wong, Experimentally feasible quantum-key-distribution scheme using qubit-like qudits and its comparison with existing qubit- and qudit-based protocols, *Phys. Rev. A* **95**, 022311 (2017).

- [45] S. Wang, Z.-Q. Yin, H. F. Chau, W. Chen, C. Wang, G.-C. Guo, and Z.-F. Han, Proof-of-principle experimental realization of a qubit-like qudit-based quantum key distribution scheme, *Quantum Sci. Technol.* **3**, 025006 (2018).
- [46] H. Bechmann-Pasquinucci and W. Tittel, Quantum cryptography using larger alphabets, *Phys. Rev. A* **61**, 062308 (2000).
- [47] N. J. Cerf, M. Bourennane, A. Karlsson, and N. Gisin, Security of Quantum Key Distribution Using d -Level Systems, *Phys. Rev. Lett.* **88**, 127902 (2002).
- [48] S. Gröblacher, T. Jennewein, A. Vaziri, G. Weihs, and A. Zeilinger, Experimental quantum cryptography with qutrits, *New J. Phys.* **8**, 75 (2006).
- [49] A. Sit, F. Bouchard, R. Fickler, J. Gagnon-Bischoff, H. Larocque, K. Heshami, D. Elser, C. Peuntinger, K. Günthner, B. Heim, C. Marquardt, G. Leuchs, R. W. Boyd, and E. Karimi, High-dimensional intracity quantum cryptography with structured photons, *Optica* **4**, 1006 (2017).
- [50] R. Fickler, F. Bouchard, E. Giese, V. Grillo, G. Leuchs, and E. Karimi, Full-field mode sorter using two optimized phase transformations for high-dimensional quantum cryptography, *J. Opt.* **22**, 024001 (2020).
- [51] I. Vagniluca, B. Da Lio, D. Rusca, D. Cozzolino, Y. Ding, H. Zbinden, A. Zavatta, L. K. Oxenløwe, and D. Bacco, Efficient Time-Bin Encoding for Practical High-Dimensional Quantum Key Distribution, *Phys. Rev. Applied* **14**, 014051 (2020).
- [52] S. Etcheverry, G. Cañas, E. S. Gómez, W. A. T. Nogueira, C. Saavedra, G. B. Xavier, and G. Lima, Quantum key distribution session with 16-dimensional photonic states, *Sci. Rep.* **3**, 2316 (2013).
- [53] G. Cañas, N. Vera, J. Cariñe, P. González, J. Cardenas, P. W. R. Connolly, A. Przysieszna, E. S. Gómez, M. Figueroa, G. Vallone, P. Villoresi, T. F. da Silva, G. B. Xavier, and G. Lima, High-dimensional decoy-state quantum key distribution over multicore telecommunication fibers, *Phys. Rev. A* **96**, 022317 (2017).
- [54] F. Xu, X. Ma, Q. Zhang, H.-K. Lo, and J.-W. Pan, Secure quantum key distribution with realistic devices, *Rev. Mod. Phys.* **92**, 025002 (2020).
- [55] A. Boaron, B. Korzh, R. Houlmann, G. Boso, D. Rusca, S. Gray, M.-J. Li, D. Nolan, A. Martin, and H. Zbinden, Simple 2.5 GHz time-bin quantum key distribution, *Appl. Phys. Lett.* **112**, 171108 (2018).
- [56] S. Ecker, F. Bouchard, L. Bulla, F. Brandt, O. Kohout, F. Steinlechner, R. Fickler, M. Malik, Y. Guryanova, and R. Ursin *et al.*, Overcoming noise in entanglement distribution, *Phys. Rev. X* **9**, 041042 (2019).
- [57] R. König and R. Renner, A de Finetti representation for finite symmetric quantum states, *J. Math. Phys.* **46**, 122108 (2005).
- [58] M. Christandl, R. König, and R. Renner, Postselection Technique for Quantum Channels with Applications to Quantum Cryptography, *Phys. Rev. Lett.* **102**, 020504 (2009).
- [59] I. Devetak and A. Winter, Distillation of secret key and entanglement from quantum states, *Proc. R. Soc. London, Ser. A* **461**, 207 (2005), arXiv:quant-ph/0306078 [quant-ph].
- [60] R. Renner, *Security of Quantum key Distribution* (Diss., Naturwissenschaften, ETH Zürich, Nr. 16242, 2006, 2005).
- [61] U. M. Maurer, Secret key agreement by public discussion from common information, *IEEE Trans. Inf. Theory* **39**, 733 (1993).
- [62] D. Gottesman and H.-K. Lo, Proof of security of quantum key distribution with two-way classical communications, *IEEE Trans. Inf. Theory* **49**, 457 (2003).
- [63] B. Kraus, C. Branciard, and R. Renner, Security of quantum-key-distribution protocols using two-way classical communication or weak coherent pulses, *Phys. Rev. A* **75**, 012316 (2007).
- [64] J. Bae and A. Acín, Key distillation from quantum channels using two-way communication protocols, *Phys. Rev. A* **75**, 012334 (2007).
- [65] X.-M. Hu, C. Zhang, Y. Guo, F.-X. Wang, W.-B. Xing, C.-X. Huang, B.-H. Liu, Y.-F. Huang, C.-F. Li, G.-C. Guo, X. Gao, M. Pivoluska, and M. Huber, Pathways for entanglement based quantum communication in the face of high noise, arXiv e-prints, arXiv:2011.03005 (2020).